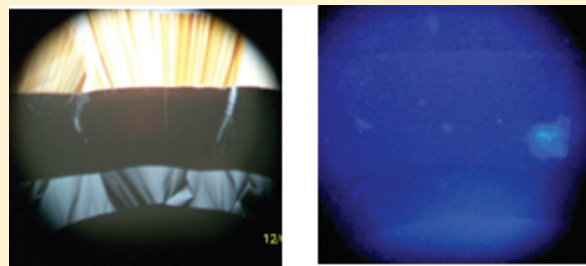


Biologically Relevant Lyotropic Liquid Crystalline Phases in Mixtures of *n*-Octyl β -D-Glucoside and Water. Determination of the Phase Diagram by Fluorescence Spectroscopy

Kerry K. Karukstis,* Whitney C. Duim, Gerald R. Van Hecke, and Nagiko Hara

Department of Chemistry, Harvey Mudd College, Claremont, California 91711, United States

ABSTRACT: When mixed with water, *n*-octyl β -D-glucoside forms self-assembled nanostructures, several of which are liquid crystalline and all of which depend on the water/glucoside ratio and temperature. For practical use of these phases, a detailed understanding of the conditions under which they exist (i.e., the isobaric phase diagram) is required. We use the fluorescence of the dye molecule prodan as a new approach to probe the phases formed in these mixtures. The prodan fluorescence signal depends on the polarity of its environment and thus the phase(s) in which the dye exists. Visual inspection of the total fluorescence signal can qualitatively determine the phases present, including coexisting phases. Temperature-induced phase changes are also detected from variations observed in the prodan fluorescence spectrum. The sensitivity of this new technique allows the single- and multiple-phase regions to be mapped carefully for the first time.



INTRODUCTION

Environmentally safe surfactants prepared from renewable resources are of great practical interest as biodegradable and nontoxic materials for pharmaceutical, cosmetic, and food preparations. The alkyl glucosides are examples of sustainable or "green" amphiphiles based on carbohydrate raw materials that are available in large quantities and at competitive prices in the world market. These glucose-based surfactants are the most important sugar surfactants today on the basis of annual production figures.¹ The commercial exploitation of alkyl glucosides became a reality only recently with the development of synthetic procedures to derivatize long-chain alcohols on a large industrial scale.^{2,3} The high rate of biodegradation, the low level of aquatic toxicity, and the favorable dermatological properties of these surfactants make them especially attractive for use in technical applications and personal care products.⁴

As with other surfactants, a key feature of amphiphilic alkyl glucosides is their ability to undergo self-assembly in water, a process in which a complex hierarchical structure is established without external intervention. Factors such as surfactant molecular structure, surfactant concentration, and temperature dictate the aggregates formed. As members of nonionic surfactants with six- or twelve-carbon sugars as the hydrophilic headgroup, alkyl glucosides exhibit an extensive range of aggregates in aqueous solution, several of which are liquid crystalline. These aggregates form as a consequence of the strong hydrogen bonds between the hydroxy groups of the sugar unit and water molecules. Applications of alkyl glucosides and the aggregates they form include drug delivery, membrane protein solubilization, catalysis, and use as model membranes. Given the technological and economic impact of alkyl glucoside surfactants in the chemical industry and particularly in the

pharmaceutical and biotechnology sectors, an understanding of the aggregates exhibited by this class of surfactants will enable both the modification of current applications to achieve improved performance and the design of new materials with enhanced properties.

Despite the known utility of alkyl glucosides, their properties and phase behavior are still not fully understood. Several investigations of the phase behavior of alkyl glucosides in water have been reported.^{5–16} Moreover, the phase diagrams that have been prepared for various glucosides often contain inaccurate and incomplete information. As small variations in solution composition can alter phase behavior, accurate identification of the phases that exist in aqueous mixtures of surfactants is essential for effective utilization of the properties of desired aggregates.

Several investigations^{6–16} have focused on determining the phase diagram of the short-chain *n*-octyl β -D-glucoside (Figure 1) in water, although each study acquired only limited

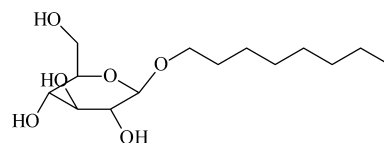


Figure 1. Chemical structure of *n*-octyl β -D-glucoside.

information to construct a partial binary surfactant–water phase diagram. These phase diagrams were constructed from a

Received: August 22, 2011

Revised: January 13, 2012

Published: March 2, 2012

combination of techniques including sorption calorimetry, deuterium NMR, polarizing microscopy, differential scanning calorimetry, rheology, and X-ray diffraction as well as visual inspection. The number of one-phase regions reported in each varies but includes an isotropic micellar solution (M) and the liquid crystalline phases hexagonal (H), cubic (C), and lamellar (L), a gel phase (G), and a “solid surfactant” phase (S). The existence or location of the gel and solid phases is either ignored or not well-defined in the published diagrams. The solid surfactant phase region typically spans a range of variable composition, and thus, this region should be more accurately denoted as a *solid solution*. In most cases, two-phase regions are not reported^{6,10} (or cited as too narrow to indicate^{7,8,13,14}), are limited in number,⁷ are incorrectly drawn,^{9,15,16} and/or are detected but not unambiguously assigned to specific phases.^{11,15}

In particular, these phase diagrams exhibit thermodynamic shortcomings to the horizontal transverse rule and the phase rule. The horizontal transverse rule states that, for any horizontal line at constant temperature in a binary phase diagram of temperature vs surfactant composition, the sequence of phases as composition is increased (or decreased) *must* (a) start and end with a homogeneous phase (i.e., one-phase region) and (b) alternate between homogeneous and heterogeneous phases. Due to the absence of all or many of the required two-phase regions in the reported phase diagrams, the horizontal transverse rule is often violated. The phase rule specifies that the number of independent intensive variables (e.g., temperature, pressure, composition of phases) or degrees of freedom (F) that must be designated to describe the state of a system completely is equal to the number of components in the system (C) plus the number of field variables (L ; e.g., temperature, pressure, gravitational field, magnetic field, etc.) minus the number of phases (P) minus the number of pre-existing or special conditions (R ; e.g., phases with identical compositions) [$F = C + L - P - R$]. For an isobaric temperature vs composition diagram (i.e., $L = 1$, only temperature can vary) of a binary (surfactant plus water) system (i.e., $C = 2$), the phase rule is $F = 3 - P - R$. The phase rule is violated in those phase diagrams where three phases are indicated to be in coexistence at a single composition and temperature point where $R = 1$ and $F = -1$.

As a novel and effective approach to characterizing phase diagrams of glucose-based surfactants, we have used fluorescence spectroscopic measurements to construct the phase diagram of the binary system of *n*-octyl β -D-glucoside (β -C₈G₁) in water. Our novel construction is achieved using the powerful spectral sensitivity of a particular fluorescence probe to the polarity of its environment. The fluorophore prodan (6-propionyl-2-(dimethylamino)naphthalene, Figure 2) is an ideal probe for examining the phase behavior of aqueous surfactant systems. Prodan's solubility in a wide range of solvents enables its distribution into an array of single-phase and multiphasic regions having different polarities.^{17–23} Furthermore, the observed fluorescence signal can be simultaneously indicative

of multiple aggregates as a consequence of the measurable fluorescence intensity in a range of solvents and the sensitivity of the wavelength of maximum emission (λ_{max}) to the polarity of prodan's environment.^{17–23} For example, the emission λ_{max} ranges from 402 nm in the nonpolar solvent cyclohexane to 522 nm in aqueous solution.^{17,19–21} The fluorescence signature of prodan in surfactant aggregates is thus a composite spectrum with contributions from the probe populations within various microdomains of the aggregate(s) present. Thus, the significant advantages of this innovative approach include (1) the use of a single technique to demarcate distinct phase regions of the binary system, (2) the application of a more generally accessible instrumental technique to the study of phase behavior, (3) the utilization of a technique with the sensitivity to identify both single-phase and multiphasic regions, and (4) the determination of a phase diagram in a more rapid and streamlined fashion.

EXPERIMENTAL SECTION

Sample Preparation and Spectroscopy. β -C₈G₁ (>99.5%, $\alpha < 0.5\%$, Anagrade) was obtained from Anatrace (Maumee, OH) and used without further purification. A 3 mM stock solution of the fluorescence probe prodan (Molecular Probes, Eugene, OR) was prepared by dissolving the prodan in dimethyl sulfoxide (DMSO; Aldrich, HPLC grade). From the stock solution 1–10 μM solutions of prodan in Milli-Q Plus Millipore-filtered water were prepared. Samples were prepared by heating weighed mixed quantities of β -C₈G₁ (approximately 800 mg of glucoside per sample) and prodan solution in quartz cuvettes with screw-cap tops (Starna Cells, Inc., Atascadero, CA; Laser Science, Inc., Newton, MA). The total volume of the samples was approximately 1 mL. Samples were heated to a homogeneous fluid phase and mixed while fluid. Viscous samples with high concentrations of β -C₈G₁ were heated and mixed repeatedly or heated at a moderate temperature (50–65 °C) for extended periods of time, 1 h to 3 days.

After a sample appeared to be fully mixed on visual inspection, the sample was allowed to sit for 1–7 days before fluorescence measurements were taken. Additional fluorescence measurements were collected over several weeks to confirm phase equilibration. For samples with compositions near phase boundaries at room temperature, separation of the mixture into two phases was often observed. Sample weights were monitored to check for any loss of water. The spectral data of any samples that lost weight were not used to construct the final phase diagram.

As a further test of the sensitivity of the method in detecting coexisting phases and the time required for prodan to enter the microregions of a sample, an 84.00 wt % β -C₈G₁ sample was prepared initially with no prodan. After the sample had been mixed and equilibrated, 0.17 μL of the 3 mM prodan stock solution was added to the top of the sample, and then the cuvette was sealed without the contents being mixed. The amount of prodan added was chosen to achieve the same final prodan concentration in the mixture as would have been present had the sample been prepared with the 3 μM prodan solution. Fluorescence spectra were then taken as a function of time at room temperature while the prodan diffused into the sample. The spectra changed in a few days to that originally obtained for the 84.00 wt % sample prepared using the diluted prodan solution.

The concentration of prodan was chosen to minimize the amount of free prodan in the samples and to promote the interaction of the probe with the aggregates present in the

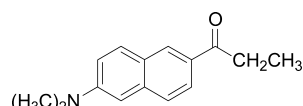


Figure 2. Chemical structure of the fluorescence probe prodan (6-propionyl-2-(dimethylamino)naphthalene).

existing phases.¹⁵ The 3 μM prodan solution produced optimal results. All of the samples were prepared with the 3 μM prodan solution except for a few high weight percent samples prepared with a 6 μM prodan solution. The final concentration of propan in the samples was 0.2–3.0 μM . A quick calculation of the typical mole fraction of propan in a 1 mL sample made with 3 μM propan solution and 800 mg of glucoside yields a result in the range of 10⁻⁶. This is easily below the impurity levels in the glucoside or the water. Thus, using the propan solution is highly unlikely to affect the determination of the phase diagram as a “third component”. Moreover, a differential scanning thermogram of the freezing point of the Millipore water used to make the mixtures is indistinguishable from that for a 3 μM propan solution made with Millipore water.

Literature phase diagrams of the $\beta\text{-C}_8\text{G}_1$ and water system guided the creation of samples such that each phase region was studied in detail. In general, simple visual observation of the sample at room temperature showed that the micellar phase was clear and fluid, the hexagonal phase was clear with a visible texture and viscous, the cubic phase was clear and viscous, the lamellar phase was cloudy and viscous, and the crystalline/gel phase was white (opaque) and viscous. However, the appearance of a sample was not a definitive indicator of the phase or phases present in the mixture.

The approximately 100 wt % sample was made by mixing $\beta\text{-C}_8\text{G}_1$ with 1 drop of 3 μM propan solution and evaporating the water. During the course of the fluorescence study from 20 to 110 °C, the appearance of the sample changed from a crystal to a gel, a gel to lamellar, and finally lamellar to a clear fluid at 54–60, 65–73, and 106–109 °C, respectively, in agreement with Dorfler and Gopfert.⁹

Fluorescence Measurements and Analyses. A Perkin-Elmer LS-50B instrument was used for the fluorescence studies. Fluorescence was induced by an excitation wavelength of 340 nm, and emission spectra were recorded in the range from 350 to 650 nm. Excitation and emission slits were set at 2.5, 5.0, or 7.5 nm depending on the intensity of the emission signal. Temperature control was achieved using a Perkin-Elmer sample holder using a circulating fluid bath or a specially designed electrically heated chamber mounted that replaced the Perkin-Elmer sample holder. The chamber was fitted with a flexible heater (Omegalux KH-202/10) that was controlled by a Temp-O-Trol TOT-VOVC unit (I²R Instruments for Research and Industry). Spectra were typically collected at 5 or 10 °C intervals with temperature equilibration times from 5 to 7 min.

Polarized and Fluorescence Microscopy. Polarized light microscopy and fluorescence microscopy were used to follow penetration studies of the glucoside by the aqueous 10 μM propan solution. The penetration method used in lyotropic systems is analogous to the contact preparation technique used in studying eutectic systems. These penetration studies were conducted by observing the fluorescence of the propan as the aqueous propan solution diffused into the sample. As the solvent diffuses into the glucoside, there is a steep concentration gradient across the contact zone from 100% aqueous propan solution to 100% glucoside, corresponding to the composition axis on the binary phase diagram. These studies were done using an Olympus Model BX40 microscope equipped with a reflected light fluorescence attachment. Excitation was provided by a Hg lamp and a fluorescence cube designed to provide UV excitation at 350 nm. The fluorescence microscope was modified slightly to conduct polarized light penetration studies. A 35 mm camera polarizing

filter was placed over the normal white light source of the microscope. A piece of polarized plastic sheet was then placed on top of the microscope slide with the sample. Polarized light observation was achieved by simply rotating the camera polarizer to achieve a crossed polars condition. When it was desired to observe the sample's fluorescence, the microscope's shield was put in place to block the normal incident light and the UV beam stop removed to illuminate the sample with 350 nm light. The fluorescence was then noted. By this simple technique the same sample region at the same temperature could be observed either under crossed polars or while fluorescing as the aqueous propan solution penetrated the sample. This technique allowed visual detection of the fluorescence colors of the micellar, hexagonal, cubic, and lamellar phases to be matched with the polarized light textures for these phases, providing confirming evidence for the assignment of the fluorescence color (λ) to specific phases.

RESULTS

Single-Phase Regions. Each lyotropic phase of the system—micellar, hexagonal, cubic, lamellar, gel, and crystal-

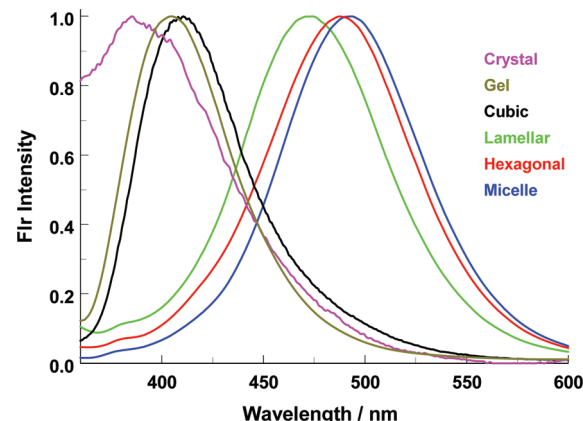


Figure 3. Propan fluorescence emission spectra observed for the aggregates exhibited by the binary system of *n*-octyl β -D-glucoside in water. The emission λ_{max} increases in the order crystal ($\lambda_{\text{max}} = 380 \text{ nm}$) < gel ($\lambda_{\text{max}} = 400 \text{ nm}$) < cubic phase ($\lambda_{\text{max}} = 410 \text{ nm}$) < lamellar phase ($\lambda_{\text{max}} = 473 \text{ nm}$) < hexagonal phase ($\lambda_{\text{max}} = 485 \text{ nm}$) < micelle ($\lambda_{\text{max}} = 490 \text{ nm}$).

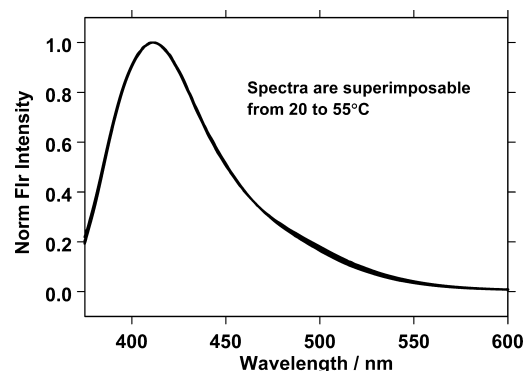


Figure 4. Normalized propan fluorescence emission spectra for a 77.07 wt % glucoside sample over the temperature range from 20 to 55 at 5 °C increments. The superimposability of the normalized spectra reflects the presence of a single type of aggregate, and the observed λ_{max} value is consistent with the cubic phase.

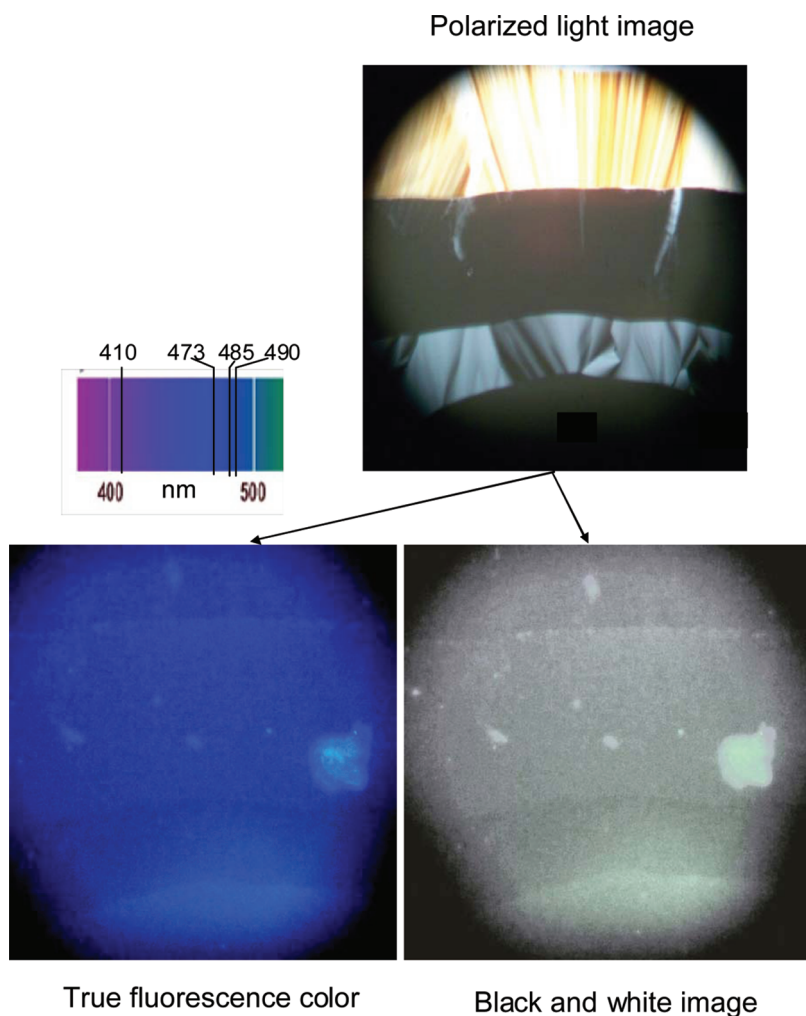


Figure 5. Penetration photomicrographs at 25 °C of *n*-octyl β-D-glucoside contacted with a 10 μM aqueous prodan solution penetrating from the bottom of the image. The top image shows (from top to bottom) the textures typical for lamellar, cubic [isotropic], hexagonal, and micellar [isotropic] phases under crossed polarizers. The bottom left image is taken as the sample fluoresces under UV excitation [338–380 nm]. The bottom right image is the left image in black and white. While the various fluorescence colors can be distinguished, the black and white image clearly shows the same regions as the crossed polars image.

line—was detected and found to yield a unique prodan fluorescence emission spectrum with a characteristic shape and peak wavelength, allowing for straightforward differentiation of the phases. Figure 3 illustrates the normalized signature fluorescence spectra of each aggregate. In general, phases with three-dimensional order (cubic, crystal) or high viscosity (gel) exhibit spectra centered at short wavelength, reflective of the probe partitioned into hydrophobic and/or constrained regions of the microstructures. The crystal and cubic phases with three-dimensional order typically show structure on the fluorescence spectra. Such structure is believed to be characteristic of these phases and originates from internal scattering or diffraction of the emitted light. The presence of this structure does not appear to affect the position of λ_{\max} . Those phases with more bilayer ordering of the aggregates (lamellar) or without fixed positioning of the aggregates within the aqueous medium (micellar) exhibit spectra with higher λ_{\max} values reflecting the positioning of prodan molecules in the hydration sphere of the aggregate. Within each grouping of structures, the higher the surfactant concentration, the shorter the observed λ_{\max} values, in other words, cubic λ_{\max} (~77 wt %) > gel λ_{\max} (~95 wt %) > crystalline λ_{\max} (~100 wt %) and similarly

micellar λ_{\max} (~52 wt %) > hexagonal λ_{\max} (~62 wt %) > lamellar λ_{\max} (~85 wt %). The spectrum shown for the crystalline phase was obtained by mixing a small amount of prodan solution with solid glucoside. (See the Experimental Section for details.) The observed spectrum is clearly not free prodan in water since the λ_{\max} in that case is 522 nm. We interpret this crystal spectrum to be representative of prodan cocrystallized with the glucoside. The structure on the spectrum characteristic of a three-dimensional organization and the position of the λ_{\max} consistent with a less polar environment for the prodan further support our interpretation.

The presence of a single aggregate in an aqueous glucoside sample over a range of temperatures would give rise to a series of superimposable normalized fluorescence spectra. Figure 4 shows such a situation for the 77.07 wt % glucoside sample from 20 to 55 °C where the spectra are attributed to the presence of the cubic phase.

The photomicrographs shown in Figure 5 are for a penetration study of *n*-octyl β-D-glucoside with 10 μM prodan in water at 25 °C. All the images are of the same region of the sample, first under crossed polars and then while fluorescing under UV excitation. Under crossed polars the textures

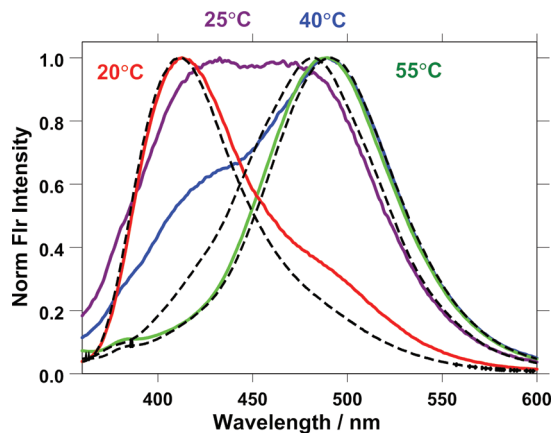


Figure 6. Fluorescence spectra observed for prodan incorporated within a 74.04 wt % sample of *n*-octyl β -D-glucoside at 20 °C (red), 25 °C (purple), 40 °C (blue), and 55 °C (green). Also included in the graph are representative spectra (black dotted curves) of the cubic (77.07 wt % at 30 °C), hexagonal (62.12 wt % at 10 °C), and micellar (51.02 wt % at 45 °C) phases. The spectra shift in shape and position as the type and/or relative amount of the aggregates present vary. As noted in the phase diagram, assignments of the surfactant aggregates present are cubic + hexagonal at 20 and 25 °C, cubic + micellar at 40 °C, and micellar at 55 °C.

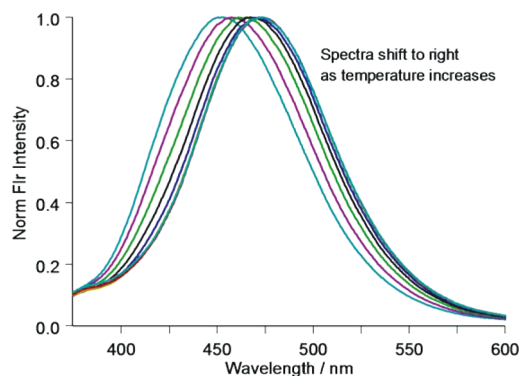


Figure 7. Fluorescence spectra observed for prodan incorporated within an 87.74 wt % sample of *n*-octyl β -D-glucoside at increasing temperature from 20 to 90 °C in 10 °C increments. The spectra red shift from 20 to 70 °C and are superimposable from 70 to 90 °C. Assignments of the surfactant aggregates present are described in the text.

characteristic of the birefringent hexagonal and lamellar phases are clearly discernible. The micellar and cubic phases are optically isotropic and thus should appear completely black. While the coexistence regions between M + H, H + C, and C + L would be expected, several factors obscure the clear observation of these regions. The birefringence of the M + H, H + C, and C + L regions could only be due to the birefringence of the H and L phases. The observation of shades of dark, not black, suggests a dilution of the birefringent phase by the isotropic phase. Further complicating the analysis is that the penetration of the prodan solution need not be uniform, leading to regions of different compositions and hence net birefringence. A conclusion must be that crossed polars images can be used to identify single birefringent regions but clear identification of coexisting regions is not possible. This difficulty limits virtually all penetration studies as also noted by Nilsson et al.¹⁴

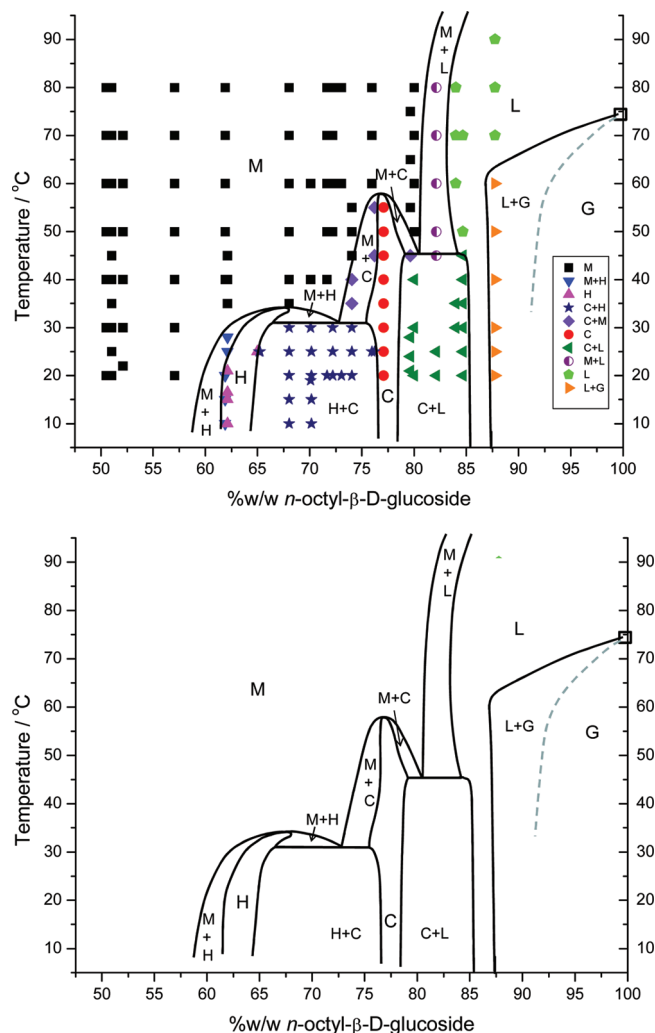


Figure 8. Isobaric temperature–composition phase diagram for *n*-octyl β -D-glucoside. The top diagram shows the actual phases at specific temperatures and compositions as determined from the fluorescence spectra, while the bottom figure is the same without the detailed points. The complex gel–solid solution behavior at low temperatures has been suppressed. Also the azeotrope-like behavior of the micelle and lamellar phases that shows a temperature–composition maximum point around 90% and 125 °C⁹ has not been drawn in to better focus on the lower temperature phases.

The different discernible fluorescence colors in the image do correspond to the typical peak wavelengths of the fluorescence signals characteristic of the lamellar, cubic, hexagonal, and micellar phases. These photomicrographs further confirm the assignment of the fluorescence signals to specific phases.

Multiphase Regions. The presence of multiple aggregates in a given aqueous glucoside sample is easily detected as a consequence of the fact that the observed prodan fluorescence spectrum is the sum of the individual prodan spectra emanating from the distinct aggregates present in the sample. Normalized fluorescence spectra of the aqueous glucoside samples reveal multiphase regions in one of two primary ways: (Case 1) Fluorescence spectra may change in shape (and possibly in λ_{max} value) as the relative contributions of the aggregates present vary as the temperature of the sample is altered. This situation is most common when the spectra of the individual aggregates have significantly separated λ_{max} values and distinct relative contributions to the overall spectrum; (Case 2) Fluorescence

spectra may exhibit similar shapes but shift in observed λ_{\max} value as the temperature of the sample is changed. This situation is most common when the distinct aggregates present have similar relative contributions to the overall spectrum.

Figure 6 illustrates case 1 where the normalized prodan fluorescence spectra change in shape and λ_{\max} value as a given glucoside sample is raised in temperature. The fluorescence spectra observed for prodan incorporated within a 74.04 wt % sample of *n*-octyl β -D-glucoside are presented at 20 °C (red), 25 °C (purple), 40 °C (blue), and 55 °C (green). Also included in the graph are representative spectra (black dotted curves) of the cubic (77.07 wt % at 30 °C), hexagonal (62.12 wt % at 10 °C), and micellar (51.02 wt % at 45 °C) phases. The spectra of the 74.04 wt % sample shift in shape and position as the type and/or relative amount of the aggregates present vary. The assignments of the surfactant aggregates present are cubic + hexagonal at 20 and 25 °C (with significantly more hexagonal phase present at 25 °C), cubic + micellar at 40 °C, and micellar at 55 °C.

Figure 7 illustrates case 2 where the shifting λ_{\max} value of the observed fluorescence spectra as temperature is increased is indicative of multiple-phase regions. Similar relative contributions of two aggregates to the overall spectrum lead to temperature-dependent spectra with similar shapes yet distinctive λ_{\max} values. The spectra presented are those collected for an 87.74 wt % sample at 10 °C increments from 20 to 90 °C. As the temperature increases, the spectra shift to longer wavelength ($\lambda_{\max} = 452, 458, 464, 468, 470$, and 473 nm from 20 to 70 °C), with those at 70–90 °C superimposable ($\lambda_{\max} = 473$ nm). A two-phase region of gel and lamellar phases is proposed to be present from 20 to 60 °C with increasing amounts of lamellar phase present at higher temperature, as reflected in the spectral red shift. A single lamellar phase is present from 70 to 90 °C, supported by the superimposable spectra with a constant λ_{\max} .

On the basis of the analysis of fluorescence from samples with surfactant compositions varying from 0 to 100 wt % over the temperature range from 5 to as high as 140 °C, we suggest that the complete phase diagram for the *n*-octyl β -D-glucoside and water system should be as shown in Figure 8. The M, H, C, L, and G phases are clearly recognized. The two-phase coexistence regions are delineated, and the zero degree of freedom three-phase coexistence temperatures (indicated by the two horizontal lines) are estimated. The three-phase coexistence lines were drawn knowing that if a region in the diagram exists where three two-phase coexistence regions occur between three phases, then there must be a three-phase invariant line connecting those three phases. The invariant line temperatures were estimated knowing the temperatures at which the other three phases exist. The diagram should be viewed as thermodynamically accurate, satisfying the criteria mentioned earlier, but semiquantitative with the indicated line temperature accurate to ± 3 °C as spectra were taken at 5 °C intervals near phase transitions and composition accurate to ± 1 wt %. The temperature accuracy of the invariant lines is probably more on the order of ± 5 °C.

Our suggested diagram agrees with previously published diagrams in recognizing the M, H, C, and L phases and exhibits the same general topology. Moreover, this diagram illustrates one of the major advantages of this sensitive fluorescence approach. In particular, our diagram shows extensive and large two-phase coexistence regions that were almost nonexistent or ignored in previous phase diagrams. These two-phase regions

are significant. In virtually all phase diagrams the composition regions for the hexagonal and cubic phases are drawn with semicircular tops. Each such "top" must really represent an azeotrope-like point. While reported previously as well, these "azeotropes" are unexplained.

CONCLUSIONS

Our results show that previously constructed phase diagrams for this system seriously misrepresent the true situation. With this new, more detailed phase diagram, it will be possible to more accurately prepare phases whose physical natures are known and to design better practical uses of the surfactant *n*-octyl β -D-glucoside and other surfactants in this class.

AUTHOR INFORMATION

Corresponding Author

*E-mail: Kerry_Karukstis@hmc.edu. Phone: (909) 607-3225. Fax: (909) 607-7577.

Notes

The authors declare no competing financial interest.

ACKNOWLEDGMENTS

This research was partially supported by an award from the Beckman Scholars Program of the Arnold and Mabel Beckman Foundation. The project described was also supported by Grant 2 R15 GM55911-02 from the National Institute of General Medical Sciences of the National Institutes of Health. Acknowledgment is also made to the donors of the Petroleum Research Fund, administered by the American Chemical Society, for partial support of this research. This material is based upon work supported by the National Science Foundation under Grants DUE-9451365, CHE-0353662, and CHE-080944. We thank Sarah Poe, Eric Hall, Courtney McQueen, and Shelley McCormack for their pioneering earlier work. Mike Wheeler and Glenn Turner assisted in the construction of the fluorometer temperature cell.

REFERENCES

- (1) Von Rybinski, W.; Hill, K. *Angew. Chem., Int. Ed.* **1998**, *37*, 1328–1345.
- (2) Luders, H. In *Nonionic Surfactants: Alkylpolyglucosides*; Balzer, D.; Luders, H., Eds.; Dekker: New York, 2000.
- (3) Lichtenthaler, F. W.; Peters, S. C. R. *Chim.* **2004**, *7*, 65–90.
- (4) Homberg, K.; Jonsson, B.; Kronberg, B.; Lindman, B. *Surfactants and Polymers in Aqueous Solution*, 2nd ed.; Wiley: New York, 2002; Chapter 1.
- (5) Guiramand, C.; Hurel, V. Foaming Composition Containing Fibers and Surfactant. U.S. Patent 20030024556, Feb 6, 2003.
- (6) Garavito, R. M.; Ferguson-Miller, S. *J. Biol. Chem.* **2001**, *276*, 32403–32406.
- (7) Kocherbitov, V.; Soderman, O.; Wadso, L. *J. Phys. Chem. B* **2002**, *106*, 2910–2917.
- (8) Hantzscher, D.; Schulte, J.; Enders, S.; Quitsch, K. *Phys. Chem. Chem. Phys.* **1999**, *1*, 895–904.
- (9) Dorfler, H.-D.; Gopfert, A. *J. Dispersion Sci. Technol.* **1999**, *20*, 35–58.
- (10) Zulauf, M. In *Crystallization of Membrane Proteins*; Michel, H., Ed.; CRC Press, Inc: Boca Raton, FL, 1991; pp 54–71.
- (11) Loewenstein, A.; Igner, D.; Zehavi, U.; Zimmermann, H.; Emerson, A.; Luckhurst, G. R. *Liq. Cryst.* **1990**, *7*, 457–474.
- (12) Loewenstein, A.; Igner, D. *Liq. Cryst.* **1991**, *10*, 457–466.
- (13) Boyd, B. J.; Drummond, C. J.; Krodkiewska, I.; Grieser, F. *Langmuir* **2000**, *16*, 7359–7367.

- (14) Nilsson, F.; Soderman, O.; Johansson, I. *Langmuir* **1996**, *12*, 902–908.
- (15) Bonicelli, M. G.; Ceccaroni, G. F.; La Mesa, C. *Colloid Polym. Sci.* **1998**, *276*, 109–116.
- (16) Sakya, P.; Seddon, J. M.; Templer, R. H. *J. Phys. II* **1994**, *4*, 1311–1331.
- (17) Karukstis, K. K. Encapsulation of Fluorophores in Multiple Microenvironments in Surfactant-Based Supramolecular Assemblies. In *Handbook of Surfaces and Interfaces of Materials, Vol. 3: Nanostructured Materials, Micelles, and Colloids*; Nalwa, H. S., Ed.; Academic Press: San Diego, CA, 2001; Chapter 12, pp 465–491.
- (18) Weber, G.; Farris, F. *J. Biochemistry* **1979**, *18*, 3075–3078.
- (19) Karukstis, K. K.; Kao, M. Y.; Savin, D. A.; Bittker, R. A.; Kaphengst, K. J.; Emetarom, C. M.; Naito, N. R.; Takamoto, D. Y. *J. Phys. Chem.* **1995**, *99*, 4339–4346.
- (20) Karukstis, K. K.; Suljak, S. W.; Waller, P. J.; Whiles, J. A.; Thompson, E. H. *Z. J. Phys. Chem.* **1996**, *100*, 11125–11132.
- (21) Karukstis, K. K.; Frazier, A. A.; Martula, D. S.; Whiles, J. A. *J. Phys. Chem.* **1996**, *100*, 11133–11138.
- (22) Karukstis, K. K.; Frazier, A. A.; Loftus, C. T.; Tuan, A. S. *J. Phys. Chem. B* **1998**, *102*, 8163–8169.
- (23) Karukstis, K. K.; McCormack, S. A.; McQueen, T. M.; Goto, K. F. *Langmuir* **2004**, *20*, 64–72.